

The $[\text{Co}_4\text{O}_4]^{4+}$ Cubane as a Quadruply-Bridging Unit: The Mixed-Valence Cluster $[\text{Co}_8\text{O}_4(\text{O}_2\text{CPh})_{12}(\text{solv})_4]$ (solv = DMF, MeCN, H_2O)

Katerina Dimitrou, Jui-Sui Sun,[†] Kirsten Folting, and George Christou*

Department of Chemistry and Molecular Structure Center, Indiana University, Bloomington, Indiana 47405-4001

Received December 13, 1994[⊗]

Synthetic procedures are described that allow access to an octanuclear, mixed-valence $4\text{Co}^{\text{II}}, 4\text{Co}^{\text{III}}$ molecular aggregate. Oxidation of $\text{Co}(\text{O}_2\text{CPh})_2$ in DMF with aqueous H_2O_2 leads to a dark emerald-green solution from which can be isolated $[\text{Co}_8\text{O}_4(\text{O}_2\text{CPh})_{12}(\text{DMF})_3(\text{H}_2\text{O})]$ (**1a**) in ~60% yield. The same reaction in MeCN leads to $[\text{Co}_8\text{O}_4(\text{O}_2\text{CPh})_{12}(\text{MeCN})_3(\text{H}_2\text{O})]$ (**1b**). Complex **1b**·2MeCN crystallizes in triclinic space group $P\bar{1}$ with the following unit cell dimensions at $-153\text{ }^\circ\text{C}$: $a = 15.056(4)\text{ \AA}$, $b = 23.548(6)\text{ \AA}$, $c = 14.697(4)\text{ \AA}$, $\alpha = 90.74(1)^\circ$, $\beta = 114.75(1)^\circ$, $\gamma = 75.12(1)^\circ$, $V = 4546.5\text{ \AA}^3$, $Z = 2$. A total of 10 207 unique data with $F > 3\sigma(F)$ were used to solve the structure, which refined to R and R_w values of 4.01 and 4.24%, respectively. The structure consists of a central $[\text{Co}^{\text{III}}_4\text{O}_4]^{4+}$ cubane unit, with each $\mu_3\text{-O}^{2-}$ ion becoming μ_4 by attachment to a Co^{II} center to give a $[\text{Co}_8\text{O}_4]^{12+}$ core; the $[\text{Co}_4\text{O}_4]^{4+}$ cubane is thus bridging the four Co^{II} ions. Twelve PhCO_2^- groups bridge the $\text{Co}^{\text{II}}, \text{Co}^{\text{III}}$ pairs, and terminal MeCN/ H_2O groups complete the peripheral ligation at the five-coordinate, high-spin Co^{II} centers. The Co^{III} centers are low-spin. Excluding differences in terminal ligation (MeCN or H_2O), the molecule has idealized T_d symmetry. Variable-temperature, solid-state magnetic susceptibility studies on **1a** have been carried out in the range 4.00–320 K. The effective magnetic moment decreases from $8.35\text{ } \mu_{\text{B}}/\text{Co}_8$ ($4.18\text{ } \mu_{\text{B}}$ per Co^{II}) at 320 K to $5.29\text{ } \mu_{\text{B}}/\text{Co}_8$ ($2.65\text{ } \mu_{\text{B}}/\text{Co}^{\text{II}}$) at 4.00 K. The data were fit to the theoretical expression for an axial symmetry Co^{II} ion undergoing zero-field splitting. The fitting parameters were $|D| = 23.5(2.0)\text{ cm}^{-1}$, $\Theta = -1.76(8)\text{ K}$, and $g = 2.05(2)$, with TIP set at $700 \times 10^{-6}\text{ cm}^3\text{ mol}^{-1}$. Low-temperature ($<20\text{ K}$) deviation between experimental and calculated μ_{eff} values is taken as evidence of weak, antiferromagnetic intra- and intermolecular interactions being present, the latter mediated by hydrogen-bonding contacts between two Co_8 units. ^1H NMR spectra recorded in $(\text{CD}_3)_2\text{CO}$, CD_2Cl_2 , or CD_3OD show only one set of paramagnetically-shifted benzoate resonances suggesting effective T_d solution symmetry and retention of the $[\text{Co}_8\text{O}_4]$ core on dissolution; this conclusion is supported by electronic spectral studies. Cyclic and differential pulse voltammetric studies show a quasi-reversible oxidation at 1.54 V vs SCE for **1c**; however, for **1a**, the oxidation appears irreversible.

Introduction

Our interest in 3d metal carboxylate chemistry has been steadily increasing over the last several years as it has become apparent that this area represents a rich source of high-nuclearity, oxide-bridged products with interesting structural, spectroscopic, and magnetic properties.¹ Although the majority of our efforts have been concentrated in Mn chemistry,² we have recently extended our interests to Co,³ believing that Co carboxylate chemistry could prove a rich area and that obtained complexes

could provide interesting comparisons and contrasts with our previous products with other metals; Co carboxylate chemistry is a relatively unexplored area for this otherwise well-explored metal.⁴ Our conviction was quickly borne out by initial results from an investigation of the oxidation of cobalt(II) acetate/2,2'-bipyridine (bpy) mixtures by aqueous H_2O_2 ;³ this and related reaction systems allowed ready access to $[\text{Co}_2(\text{OH})_2(\text{OAc})_3(\text{bpy})_2](\text{ClO}_4)$, $[\text{Co}_3\text{O}(\text{OH})_3(\text{OAc})_2(\text{bpy})_3](\text{ClO}_4)_2$, and $[\text{Co}_4\text{O}_4(\text{OAc})_2(\text{bpy})_4](\text{ClO}_4)_2$, the last two complexes representing initial examples of the $[\text{Co}_3(\mu_3\text{-O})(\mu\text{-OH})_3]^{4+}$ and cubane-like $[\text{Co}_4(\mu_3\text{-O})_4]^{4+}$ cores.

The present work is an extension of the above studies and describes the result of carrying out the oxidation of cobalt(II) benzoate in DMF or MeCN with aqueous H_2O_2 in the absence of bpy or any other potentially chelating group. Under these conditions, assembly of an unusual higher-nuclearity product occurs. Herein are described the structure and properties of $[\text{Co}_8\text{O}_4(\text{O}_2\text{CPh})_{12}(\text{solv})_4]$ (**1**; solv = MeCN, DMF, H_2O) which represents the initial example of the interesting $[\text{M}_8(\mu_4\text{-O})_4]$ core in a molecular species. Portions of this work were previously communicated.⁵

[†] Department of Chemistry, Michigan State University.

[⊗] Abstract published in *Advance ACS Abstracts*, July 1, 1995.

- Hendrickson, D. N.; Christou, G.; Schmitt, E. A.; Libby, E.; Bashkin, J. S.; Wang, S.; Tsai, H.-L.; Vincent, J. B.; Boyd, P. D. W.; Huffman, J. C.; Folting, K.; Li, Q.; Streib, W. E. *J. Am. Chem. Soc.* **1992**, *114*, 2455. McCusker, J. K.; Vincent, J. B.; Schmitt, E. A.; Mino, M. L.; Shin, K.; Coggin, D. K.; Hagen, P. M.; Huffman, J. C.; Christou, G.; Hendrickson, D. N. *J. Am. Chem. Soc.* **1991**, *113*, 3012. Christou, G.; Perlepes, S. P.; Folting, K.; Huffman, J. C.; Webb, R. J.; Hendrickson, D. N. *J. Chem. Soc., Chem. Commun.* **1990**, 746.
- Sessoli, R.; Tsai, H.-L.; Schake, A. R.; Wang, S.; Vincent, J. B.; Folting, K.; Gatteschi, D.; Christou, G.; Hendrickson, D. N. *J. Am. Chem. Soc.* **1993**, *115*, 1804. Wang, S.; Tsai, H.-L.; Streib, W. E.; Christou, G.; Hendrickson, D. N. *J. Chem. Soc., Chem. Commun.* **1992**, 677. Goldberg, D. P.; Caneschi, A.; Lippard, S. J. *J. Am. Chem. Soc.* **1993**, *115*, 9299. Wemple, M. W.; Tsai, H.-L.; Streib, W. E.; Hendrickson, D. N.; Christou, G. *J. Chem. Soc., Chem. Commun.* **1994**, 1031.
- Dimitrou, K.; Folting, K.; Streib, W. E.; Christou, G. *J. Am. Chem. Soc.* **1993**, *115*, 6432.

(4) Buckingham, D. A.; Clark, C. R. In *Comprehensive Coordination Chemistry*; Wilkinson, G., Gillard, R. D., McCleverty, J. A., Eds.; Pergamon Press: Oxford, U.K., 1987; Vol. 4, p 635. West, B. O. *Polyhedron* **1989**, *8*, 3, 219.

(5) Dimitrou, K.; Folting, K.; Streib, W. E.; Christou, G. *J. Chem. Soc., Chem. Commun.* **1994**, 1385.

Table 1. Crystallographic Data for [Co₈O₄(O₂CPh)₁₂(MeCN)₃(H₂O)]·2MeCN (**1b**)

C ₉₄ H ₇₇ N ₅ O ₂₉ Co ₈ ^a	<i>f</i> w ^a = 2212.12
<i>a</i> = 15.056(4) Å	space group: <i>P</i> $\bar{1}$
<i>b</i> = 23.548(6) Å	<i>T</i> = -153 °C
<i>c</i> = 14.697(4) Å	λ = 0.71069 Å ^b
α = 90.74(1)°	ρ_{calc} = 1.616 g cm ⁻³
β = 114.75(1)°	μ = 15.018 cm ⁻¹
γ = 75.12(1)°	<i>R</i> (<i>F</i>) ^c = 0.0401
<i>V</i> = 4546.5 Å ³	<i>R</i> _w (<i>F</i>) ^d = 0.0424
<i>Z</i> = 2	

^a Including solvate molecules. ^b Graphite monochromator. ^c *R* = $\sum ||F_o| - |F_c|| / \sum |F_o|$. ^d *R*_w = $[\sum w(|F_o| - |F_c|)^2 / \sum w|F_o|^2]^{1/2}$ where *w* = $1/\sigma^2(|F_o|)$.

Experimental Section

Syntheses. All manipulations were performed under aerobic conditions using chemicals as received (Alfa).

[Co₈O₄(O₂CPh)₁₂(DMF)₃(H₂O)] (1a**).** Cobalt(II) benzoate (6.02 g, 20.0 mmol) was partially dissolved in DMF (200 mL), with stirring and gentle warming, to give a purple solution and undissolved material. To this slurry was added aqueous H₂O₂ (50%, 10 mL, 160 mmol), which caused a slow color change to dark green and further dissolution of solid. The solution was stirred at ambient temperature for 4 h, and it was then filtered and the filtrate evaporated to dryness under vacuum and with gentle heating. The resultant green, crystalline residue was slurried with cold MeCN (10 mL), and the crystals were collected by filtration, washed with MeCN, and dried under vacuum. The yield was ~60%. Anal. Calcd (found) for C₉₃H₈₃N₃O₃₂Co₈: C, 50.16 (50.03); H, 3.76 (3.73); N, 1.89 (2.03).

[Co₈O₄(O₂CPh)₁₂(MeCN)₃(H₂O)]·2MeCN (1b**·2MeCN). Method A.** The above reaction was performed in MeCN to give the same dark green solution. This was filtered (most of the Co(O₂CPh)₂ remains undissolved) and the filtrate allowed to stand undisturbed at room temperature overnight. Well-formed, X-ray-quality crystals of **1b**·2MeCN slowly appeared (and were kept in contact with the mother liquor when the crystallographic sample was being sought). The dark green crystals were collected by filtration, washed with a little cold MeCN, and dried *in vacuo*. The yield was ~12%. Drying **1b**·2MeCN *in vacuo* causes loss of both lattice and bound MeCN groups, the solid analyzing for [Co₈O₄(O₂CPh)₁₂(MeCN)(H₂O)₃] (**1c**). Anal. Calcd (found) for C₈₆H₆₉NO₃₁Co₈: C, 49.57 (49.67); H, 3.34 (3.31); N, 0.67 (0.70). Selected IR data (KBr pellet, cm⁻¹) for **1b**: 3632 (m), 3065 (w), 1597 (s), 1557 (vs), 1493 (m), 1447 (m), 1410 (vs, br), 1179 (m), 1071 (m), 1026 (m), 847 (w), 812 (w), 716 (s), 686 (s), 632 (s), 612 (m), 492 (m, br). Conductivity (25 °C): 24 and 1 S cm² mol⁻¹ in MeOH and acetone, respectively.

Method B. A higher yield of complex **1b** (and **1c**) can be obtained by following the procedure for **1a** until the point where the DMF is removed *in vacuo* to give a green, microcrystalline residue. The latter was then extracted into a minimum amount of warm CH₂Cl₂ (600 mL), and MeCN (600 mL) was added. Evaporation to almost dryness under vacuum gave microcrystalline material. The product was collected as in method A. The yield was typically >55%. Spectroscopic examination confirmed the absence of DMF and the identity of the material as complex **1c**.

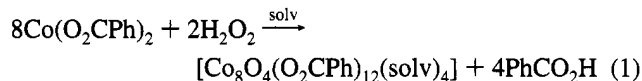
X-ray Crystallography. Data for complex **1b**·2MeCN were collected on a Picker four-circle diffractometer at -153 °C; details of the diffractometry, low-temperature facilities, and computational procedures employed by the Molecular Structure Center are available elsewhere.⁶ Data collection parameters are listed in Table 1. A green-black crystal of suitable size (0.20 × 0.35 × 0.40 mm) was affixed to a glass fiber with silicone grease and transferred to a goniostat where it was cooled to -153 °C for characterization and data collection. A systematic search of a limited hemisphere of reciprocal space revealed Laue symmetry consistent with a triclinic unit cell. The choice of the centrosymmetric space group *P* $\bar{1}$ was confirmed by the successful solution and refinement of the structure. A total of 18 886 reflections were collected (+*h*, ±*k*, ±*l*; 6° ≤ 2θ ≤ 45°); data processing produced

a unique set of 11 881 intensities and gave a residual of 0.036 for the averaging of 5912 reflections measured more than once. Four standards measured every 400 reflections showed no significant trends. No correction for absorption was performed. The structure was solved by locating the eight Co atoms in the best solution from MULTAN78. The remaining non-hydrogen atoms were obtained from subsequent iterations of least-squares refinement and difference Fourier map calculations phased on the already-located atoms. All of the non-hydrogen atoms were refined with anisotropic thermal parameters. In the final cycles of least-squares refinement, hydrogen atoms were included in fixed, calculated positions, except on O(127) and on the lattice solvent molecules. The final *R*(*F*) was 0.0401 using all of the unique data; *R*_w(*F*) was 0.0424. Reflections having *F* < 3.0σ(*F*) were given zero weight. The total number of parameters varied was 1226 (including the scale factor and an overall isotropic extinction parameter). The final difference Fourier map was essentially featureless, the largest peak being 0.63 e/Å³.

Other Measurements. Infrared (KBr pellet) and solution electronic spectra were recorded on Nicolet 510P FT-IR and Hewlett-Packard spectrophotometers, respectively. ¹H NMR data were recorded on a Varian XL-300 spectrometer; chemical shifts are quoted on the δ scale (shifts downfield are positive) and referenced versus internal HMDS. Elemental analyses were performed by Atlantic Microlab, Inc. Conductivity measurements were performed at room temperature on a 1.0 mM solution employing a YSI31A conductance bridge and a YSI3403 dip cell. Variable-temperature magnetic susceptibility data were obtained using a Quantum Design MPMS SQUID susceptometer at Michigan State University. Measurements were made with an applied magnetic field of 0.1 T (1000 G) in the temperature range 4.00–320 K. The diamagnetic correction was estimated using Pascal's constants and subtracted from the experimental data to yield the molar paramagnetic susceptibility of the compound. The data were then fitted to the appropriate theoretical expression using a least-squares-fitting procedure. Electrochemical studies were performed using a BAS Model CV-50W instrument, a standard three-electrode assembly (glassy carbon working, Pt wire auxiliary, SCE reference) and NBu₄⁺ClO₄⁻ or NBu₄⁺PF₆⁻ as supporting electrolyte. Cyclic voltammetry (CV) and differential pulse voltammetry (DPV) were carried out at scan rates of 100 and 5 mV/s, respectively.

Results

Synthesis. The use of DMF as the reaction solvent was necessitated by the low solubility of anhydrous Co(O₂CPh)₂ in most organic solvents; even in DMF, however, this compound has only moderate solubility. Addition of an excess of aqueous H₂O₂ leads to generation of a dark emerald-green color and the subsequent isolation of [Co₈O₄(O₂CPh)₁₂(DMF)₃(H₂O)] (**1a**) in good yield (~60%). Its formation is summarized in eq 1. The



analogous reaction in MeCN is hampered by the low solubility of Co(O₂CPh)₂, and the low yield of subsequent product (~12%) is primarily due to only partial dissolution and reaction of Co(O₂CPh)₂. Nevertheless, this method did give well-formed, single crystals of [Co₈O₄(O₂CPh)₁₂(MeCN)₃(H₂O)]·2MeCN (**1b**·2MeCN) suitable for crystallography. A combination of DMF as the initial reaction medium and MeCN as the final crystallization solvent (method B) allows much more satisfactory yields of **1b** (~55%) to be achieved. The product is air-stable, although **1b** loses MeCN on drying *in vacuo* and the product appears to be hygroscopic, analyzing for [Co₈O₄(O₂CPh)₁₂(MeCN)(H₂O)₃] (**1c**).

Charge considerations necessitate a 4Co^{II}, 4Co^{III} description for **1**: the presence of Co^{II} in the product of a reaction employing an excess of H₂O₂ suggests the Co^{II} centers in **1** are resistant to oxidation and that, once formed, **1** maintains its octanuclear structure in solution (*vide infra*).

(6) Chisholm, M. H.; Foltling, K.; Huffman, J. C.; Kirkpatrick, C. C. *Inorg. Chem.* **1984**, *23*, 1021.

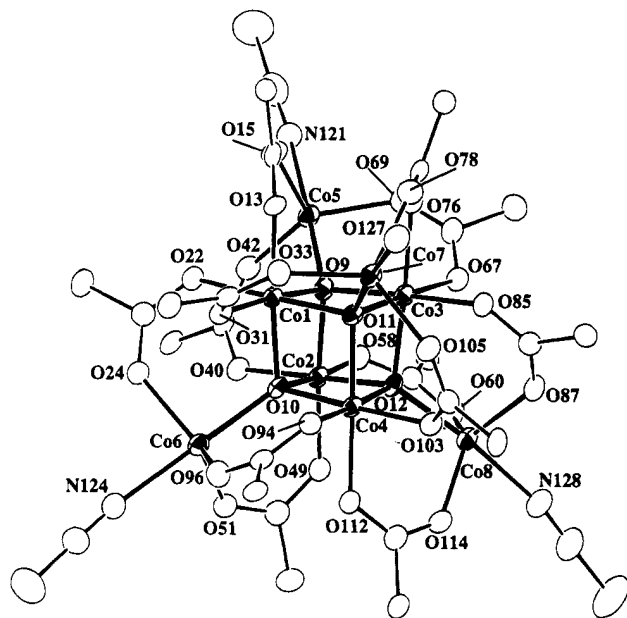


Figure 1. ORTEP representation of complex **1b** at the 50% probability level. The phenyl rings of the benzoate ligands have been omitted for clarity.

Description of Structure. A labeled ORTEP plot of **1b** is given in Figure 1, and a stereopair, in Figure 2; selected fractional coordinates and bond distances and angles are listed in Tables 2 and 3. Complex **1b**·2MeCN crystallizes in the triclinic space group $P\bar{1}$ with the asymmetric unit containing the entire molecule and two lattice MeCN groups. The structure is extremely unusual and contains a $[\text{Co}_8\text{O}_4]^{12+}$ core comprised of a $[\text{Co}_4\text{O}_4]$ inner cubane to which four additional Co atoms, Co(5)–Co(8), are attached by bonding to the oxygen atoms, O(9)–O(12). The latter are thus μ_4 and possess trigonal pyramidal geometry,⁷ with the outer Co atoms at the apices. There are twelve PhCO_2^- groups, each bridging between an outer and a cubane Co atom; the PhCO_2^- groups are in their familiar *syn,syn*-bridging mode. A terminal MeCN group on Co(5), Co(6), and Co(8) and a terminal H_2O group, O(127), on Co(7) complete five-coordination at the outer Co atoms, which possess distorted trigonal bipyramidal geometry; this is an extremely rare Co coordination number for predominantly O ligands.^{8,9} The Co^{II} ions have virtual C_{3v} symmetry with oxides and terminal MeCN or H_2O molecules lying on the axes. As expected, Co^{II} –oxide distances are significantly shorter (by ~ 0.15 Å) than the terminal Co^{II} –MeCN(H_2O) bonds. The metal atoms lie out of the equatorial planes by 0.16–0.22 Å toward their bound oxide ions. The cubane Co atoms are six-coordinate with distorted octahedral geometry.

Inspection of the structural parameters leads to the conclusion that the molecule is trapped-valence, with the cubane and outer Co atoms being the Co^{III} and Co^{II} centers, respectively. For the Co^{III} ions, the Co^{III} –oxide and Co^{III} –carboxylate bonds are in the fairly narrow ranges of 1.877(3)–1.896(3) and 1.913(3)–1.943(3) Å, respectively, values consistent with a low-spin configuration, as expected. For the Co^{II} ions, the Co^{II} –oxide (2.006(3)–2.012(3) Å) and Co^{II} –carboxylate (1.972(3)–2.027-

(3) Å) distances are significantly longer (especially since the coordination number has decreased).

If the differences in terminal ligation (MeCN vs H_2O) and the slight non-planarity of the bridging PhCO_2^- planes are ignored, the entire molecule and the $[\text{Co}_4\text{O}_4]^{4+}$ cubane core both have idealized T_d symmetry, as further emphasized by the narrow range in cubane Co^{III} – Co^{III} distances (2.809(1)–2.842(1) Å). This is to be contrasted with the only previous example of a complex with a $[\text{Co}_4\text{O}_4]^{4+}$ cubane core, $[\text{Co}_4\text{O}_4(\text{O}_2\text{CC}_6\text{H}_4\text{-}p\text{-Me})_2(\text{bpy})_4](\text{ClO}_4)_2$ (**2**),³ whose entire cation and $[\text{Co}_4\text{O}_4]^{4+}$ core both have idealized D_{2d} symmetry: the Co^{III} – Co^{III} distances in the latter fall into two distinct groups, with values of 2.845(2)–2.865(2) and 2.663(2)–2.666(2) Å. The volumes of the $[\text{Co}_4\text{O}_4]$ cubanes in **1b** and **2** are only slightly different, 7.005 and 6.869 Å³, respectively.

It is interesting that products obtained from DMF (**1a**) and MeCN (**1b**) both contain a single terminally-coordinated H_2O molecule rather than a fourth DMF or MeCN group. The reason appears to lie in the packing arrangement of the $[\text{Co}_8\text{O}_4(\text{O}_2\text{-CPh})_{12}(\text{MeCN})_3(\text{H}_2\text{O})]$ molecules in the lattice. In Figure 3 is shown that the complex packs as dimers of octanuclear units held together by hydrogen-bonding interactions between the H_2O molecule, O(127), and carboxylate oxygen O(33) in the other molecule, and *vice versa* (O(127)–O(33) = 2.856(5) Å). In addition, O(127) forms a second hydrogen-bond to one of the two lattice MeCN groups associated with each Co_8 unit (O(127)–N(133) = 3.038(5) Å). In fact, close examination of the final difference Fourier map revealed two peaks (H_a and H_b) assignable to H atoms in positions consistent with the above conclusions (O(127)– H_a –O(33) = 149.37° and O(127)– H_b –N(133) = 154.57°). These hydrogen-bonding interactions are the probable reason that **1a** and **1b** possess one bound H_2O molecule.

Although the $[\text{Co}_4\text{O}_4]^{4+}$ cubane unit has been obtained once before in complex **2**, the $[\text{Co}_8(\mu_4\text{-O})_4]^{12+}$ unit is unprecedented. In fact, the $[\text{M}_8(\mu_4\text{-O})_4]$ unit is unknown for any metal in a homometallic molecular complex, although it is known as a recognizable subunit of the extended lattice of $\text{Pb}_9\text{O}_4\text{Br}_{10}$ and related $\text{TiPb}_8\text{O}_4\text{Br}_9$.^{10a} These compounds contain $[\text{Pb}_8(\mu_4\text{-O})_4]^{8+}$ units, structurally analogous to the $[\text{Co}_8(\mu_4\text{-O})_4]^{12+}$ core of **1b**, that are then interconnected into a 3D lattice by bridging Br^- and either Ti^+ or additional Pb^{2+} ions. A heterometallic complex related to **1b** is $\text{Zn}_4\text{V}_4(\text{O}_2\text{CPh})_{12}(\text{THF})_4$,^{10b} which contains a $[\text{V}_4\text{O}_4]^{4+}$ cubane unit to which are attached four Zn^{2+} ions to give a $[\text{Zn}_4\text{V}_4(\mu_4\text{-O})_4]^{12+}$ core analogous to that in **1b**.

Magnetic Susceptibility Studies. Variable-temperature, solid-state magnetic susceptibility studies were performed on powdered samples of complex **1a** in the temperature range 4.00–320 K. The effective magnetic moment (μ_{eff}) per Co_8 molecule decreases gradually from 8.35 μ_B at 320 K to 7.84 μ_B at 79.9 K and then decreases more rapidly to 5.29 μ_B at 4.00 K. On the basis of the above structural discussion, the only unpaired electrons will be on the Co^{II} centers, since the Co^{III} ions are low-spin (t_{2g}^6 , $S = 0$). From a magnetic viewpoint, the complex is effectively tetranuclear, and the above μ_{eff} values thus translate into 4.18 μ_B/Co at 320 K and 2.65 μ_B/Co at 4.00 K (Figure 4). The 320 K value is near that expected for a high-spin ($S = 3/2$) Co^{II} ion (spin-only value 3.87 μ_B); the high-spin nature is as expected, given the predominantly weak-field carboxylate O donor atoms in the equatorial plane of the Co^{II} . Introduction of stronger-field N donors (Schiff bases, substituted imidazoles, etc.) into the equatorial and axial positions of five-coordinate Co^{II} complexes has been shown to occasionally give

(7) Peng, S.-M.; Lin, Y.-N. *Acta Crystallogr.* **1986**, C42, 1725.
 (8) (a) Holmes, R. R. *Prog. Inorg. Chem.* **1984**, 32, 119. (b) Morassi, R.; Bertini, I.; Sacconi, L. *Coord. Chem. Rev.* **1973**, 11, 343.
 (9) (a) Bertini, I.; Dapporto, P.; Gatteschi, D.; Scozzafava, A. *Inorg. Chem.* **1975**, 14, 1639. (b) Coyle, B. A.; Ibers, J. A. *Inorg. Chem.* **1970**, 9, 767. (c) Lewis, J.; Nyholm, R. S.; Rodley, G. A. *Nature (London)* **1965**, 207, 72. (d) Powling, P.; Robertson, G. B.; Rodley, G. A. *Nature (London)* **1965**, 207, 73.

(10) (a) Keller, H.-L. *Angew. Chem., Int. Ed. Engl.* **1983**, 22, 324. (b) Cotton, F. A.; Duraj, S. A.; Roth, W. J. *Inorg. Chem.* **1984**, 23, 4042.

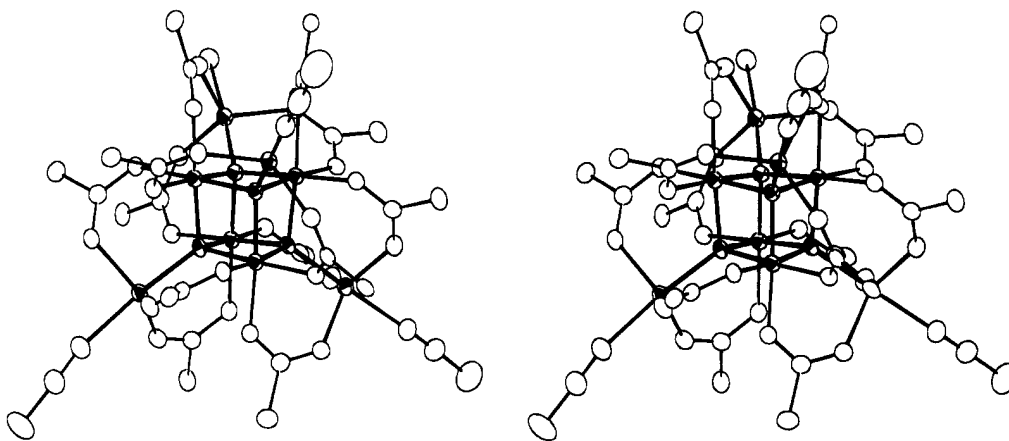


Figure 2. Stereoview of complex 1b.

Table 2. Selected Fractional Coordinates ($\times 10^4$) and Equivalent Isotropic Thermal Parameters ($\times 10^3$)^a for Complex 1b·2MeCN

atom	x	y	z	$B_{eq}, \text{\AA}^2$	atom	x	y	z	$B_{eq}, \text{\AA}^2$
Co(1)	5867.9(4)	2785.6(2)	6506.5(4)	14	C(61)	8163(4)	170(2)	5709(3)	21
Co(2)	7361.7(4)	1692.6(2)	7064.6(4)	14	O(67)	7321(2)	1781(1)	4658(2)	18
Co(3)	7019.0(4)	2438.3(2)	5392.0(4)	15	C(68)	6679(3)	1550(2)	4020(3)	19
Co(4)	7956.0(4)	2757.8(2)	7353.8(4)	14	O(69)	5855(2)	1507(1)	4001(2)	20
Co(5)	5230.8(4)	1729.3(3)	4976.2(4)	16	C(70)	6940(3)	1315(2)	3183(3)	20
Co(6)	7128.1(4)	2394.6(3)	9013.2(4)	17	O(76)	5879(2)	2788(1)	4143(2)	16
Co(7)	6379.8(4)	3904.3(2)	5618.8(4)	16	C(77)	5520(3)	3315(2)	3745(3)	18
Co(8)	9444.8(4)	1623.6(3)	6711.9(4)	17	O(78)	5669(2)	3776(1)	4169(2)	21
O(9)	6260(2)	2122(1)	5892(2)	15	C(79)	4847(3)	3395(2)	2638(3)	25
O(10)	7090(2)	2403(1)	7628(2)	15	O(85)	7795(2)	2806(1)	4960(2)	17
O(11)	6772(2)	3055(1)	6158(2)	15	C(86)	8713(3)	2615(2)	5089(3)	18
O(12)	8090(2)	2087(1)	6643(2)	14	O(87)	9351(2)	2133(1)	5581(2)	20
O(13)	4701(2)	3201(1)	5325(2)	16	C(88)	9063(3)	3010(2)	4602(3)	20
C(14)	4054(3)	2998(2)	4631(3)	19	O(94)	7751(2)	3463(1)	8017(2)	17
O(15)	4078(2)	2466(1)	4509(2)	20	C(95)	7790(3)	3481(2)	8886(3)	19
C(16)	3138(3)	3459(2)	3886(3)	20	O(96)	7617(2)	3114(1)	9360(2)	21
O(22)	4960(2)	2462(1)	6829(2)	17	C(97)	8095(3)	3995(2)	9439(3)	18
C(23)	4987(3)	2379(2)	7690(3)	18	O(103)	8843(2)	3089(1)	7020(2)	16
O(24)	5689(2)	2404(1)	8529(2)	21	C(104)	8667(3)	3613(2)	6656(3)	18
C(25)	4074(3)	2248(2)	7724(3)	20	O(105)	7802(2)	3979(1)	6163(2)	20
O(31)	5576(2)	3436(1)	7226(2)	17	C(106)	9590(3)	3826(2)	6855(3)	20
C(32)	5387(3)	3987(2)	7033(3)	18	O(112)	9161(2)	2440(1)	8604(2)	19
O(33)	5513(2)	4241(1)	6351(2)	20	C(113)	10037(3)	2162(2)	8684(3)	20
C(34)	4961(3)	4358(2)	7661(3)	23	O(114)	10243(2)	1848(1)	8071(2)	21
O(40)	6586(2)	1328(1)	7527(2)	17	C(115)	10928(3)	2237(2)	9601(3)	23
C(41)	5910(3)	1078(2)	6999(3)	16	N(121)	4070(3)	1347(2)	3992(3)	22
O(42)	5408(2)	1143(1)	6056(2)	20	C(122)	3352(4)	1251(3)	3484(4)	38
C(43)	5720(3)	641(2)	7590(3)	19	C(123)	2403(6)	1118(4)	2790(5)	68
O(49)	8566(2)	1294(1)	8229(2)	18	N(124)	7165(3)	2425(2)	10508(3)	24
C(50)	8750(3)	1312(2)	9149(3)	20	C(125)	7271(4)	2536(2)	11292(4)	26
O(51)	8184(2)	1629(1)	9511(2)	21	C(126)	7424(5)	2677(3)	12297(4)	46
C(52)	9745(3)	911(2)	9899(3)	21	O(127)	6070(2)	4817(1)	5058(2)	22
O(58)	7523(2)	1005(1)	6368(2)	17	N(128)	10923(3)	1087(2)	6929(3)	25
C(59)	8260(3)	733(2)	6195(3)	18	C(129)	11728(4)	792(2)	7196(4)	32
O(60)	9072(2)	870(1)	6396(2)	21	C(130)	12775(5)	420(3)	7530(6)	57

$$^a B_{eq} = (4/3)\sum\sum B_{ij}a_i a_j$$

high-spin/low-spin crossover,^{11–15} but the latter behavior is not expected with the present ligands and would also give a distinctly different μ_{eff} vs T plot than observed here.

The μ_{eff} vs T behavior shown in Figure 4 may be interpreted as reflecting zero-field splitting (ZFS) of the quartet ground state,¹⁷ intramolecular exchange interactions between the four

Co^{II} centers mediated by the central [Co₄O₄] “bridging” unit, intermolecular exchange interactions mediated by the hydrogen-bonding interactions, or a combination of these. The last two effects are not expected to be significant, given the large separations between magnetic orbitals involved, but they are nevertheless presumably non-zero. In contrast, ZFS for high-spin, five-coordinate Co^{II} complexes is relatively large and likely to be the dominant effect of the three. Indeed, the μ_{eff} vs T behavior of Figure 4 is qualitatively and quantitatively very similar to that observed for several mononuclear, five-coordinate Co^{II} systems,^{13–16} suggesting that ZFS is dominant by far over exchange interactions.

(11) (a) König, E. *Struct. Bonding (Berlin)* **1991**, 76, 52. (b) Gütllich, P. *Struct. Bonding (Berlin)* **1981**, 44, 83.

(12) Zarembowitch, J.; Kahn, O. *Inorg. Chem.* **1984**, 23, 589.

(13) Thuéry, P.; Zarembowitch, J. *Inorg. Chem.* **1986**, 25, 2001.

(14) Kennedy, B. J.; Murray, K. S. *Inorg. Chim. Acta* **1987**, 134, 249.

(15) Kennedy, B. J.; Fallon, G. D.; Gatehouse, B. M. K. C.; Murray, K. S. *Inorg. Chem.* **1984**, 23, 580.

(16) Rudolf, M. F.; Wolny, J. A.; Lis, T.; Starynowicz, P. *J. Chem. Soc., Dalton Trans.* **1992**, 2079.

(17) (a) Hitchman, M. A. *Inorg. Chim. Acta* **1978**, 26, 237. (b) Hitchman, M. A. *Inorg. Chem.* **1985**, 16, 1977.

Table 3. Selected Interatomic Distances (Å) and Angles (deg) for Complex **1b**

Co(1)•Co(2)	2.809(1)	Co(1)•Co(5)	3.382(1)	Co(2)•Co(4)	2.842(1)	Co(3)•Co(5)	3.364(1)
Co(1)•Co(3)	2.823(1)	Co(2)•Co(8)	3.351(1)	Co(3)•Co(4)	2.820(1)	Co(4)•Co(8)	3.417(1)
Co(1)•Co(4)	2.838(1)	Co(2)•Co(6)	3.388(1)	Co(3)•Co(8)	3.369(1)	Co(4)•Co(7)	3.353(1)
Co(1)•Co(7)	3.348(1)	Co(2)•Co(5)	3.368(1)	Co(3)•Co(7)	3.389(1)	Co(4)•Co(6)	3.373(1)
Co(1)•Co(6)	3.370(1)	Co(2)•Co(3)	2.824(1)				
Co(1)–O(9)	1.881(3)	Co(2)–O(58)	1.922(3)	Co(4)–O(103)	1.930(3)	Co(6)–N(124)	2.174(4)
Co(1)–O(10)	1.888(3)	Co(3)–O(9)	1.885(3)	Co(4)–O(112)	1.943(3)	Co(7)–O(11)	2.006(3)
Co(1)–O(11)	1.884(3)	Co(3)–O(11)	1.882(3)	Co(5)–O(9)	2.007(3)	Co(7)–O(33)	2.027(3)
Co(1)–O(13)	1.915(3)	Co(3)–O(12)	1.880(3)	Co(5)–O(15)	1.995(3)	Co(7)–O(78)	2.004(3)
Co(1)–O(22)	1.940(3)	Co(3)–O(67)	1.942(3)	Co(5)–O(42)	2.002(3)	Co(7)–O(105)	2.003(3)
Co(1)–O(31)	1.913(3)	Co(3)–O(76)	1.915(3)	Co(5)–O(69)	2.016(3)	Co(7)–O(127)	2.174(3)
Co(2)–O(9)	1.880(3)	Co(3)–O(85)	1.916(3)	Co(5)–N(121)	2.147(4)	Co(8)–O(12)	2.012(3)
Co(2)–O(10)	1.884(3)	Co(4)–O(10)	1.889(3)	Co(6)–O(10)	2.012(3)	Co(8)–O(60)	1.988(3)
Co(2)–O(12)	1.886(3)	Co(4)–O(11)	1.877(3)	Co(6)–O(24)	1.972(3)	Co(8)–O(87)	1.998(3)
Co(2)–O(40)	1.938(3)	Co(4)–O(12)	1.896(3)	Co(6)–O(51)	1.976(3)	Co(8)–O(114)	2.001(3)
Co(2)–O(49)	1.915(3)	Co(4)–O(94)	1.936(3)	Co(6)–O(96)	1.993(3)	Co(8)–N(128)	2.150(4)
O(9)–Co(1)–O(10)	82.86(12)	O(9)–Co(3)–O(12)	82.44(12)	O(9)–Co(5)–O(69)	97.33(11)	O(12)–Co(8)–N(128)	174.29(14)
O(9)–Co(1)–O(11)	82.46(12)	O(9)–Co(3)–O(67)	96.97(12)	O(9)–Co(5)–N(121)	177.11(13)	O(60)–Co(8)–O(87)	117.52(13)
O(9)–Co(1)–O(13)	96.41(12)	O(9)–Co(3)–O(76)	94.63(12)	O(15)–Co(5)–O(42)	120.53(13)	O(60)–Co(8)–O(114)	127.33(13)
O(9)–Co(1)–O(22)	93.86(12)	O(9)–Co(3)–O(85)	175.36(12)	O(15)–Co(5)–O(69)	114.19(13)	O(60)–Co(8)–N(128)	83.01(13)
O(9)–Co(1)–O(31)	175.25(12)	O(11)–Co(3)–O(12)	82.62(12)	O(15)–Co(5)–N(121)	82.51(14)	O(87)–Co(8)–O(114)	113.14(13)
O(10)–Co(1)–O(11)	81.76(12)	O(11)–Co(3)–O(67)	177.38(12)	O(42)–Co(5)–O(69)	122.18(13)	O(87)–Co(8)–N(128)	91.26(14)
O(10)–Co(1)–O(13)	174.85(11)	O(11)–Co(3)–O(76)	96.47(12)	O(42)–Co(5)–N(121)	85.29(13)	O(114)–Co(8)–N(128)	82.44(14)
O(10)–Co(1)–O(22)	97.70(12)	O(11)–Co(3)–O(85)	93.04(12)	O(69)–Co(5)–N(121)	84.52(13)	Co(1)–O(9)–Co(2)	96.64(13)
O(10)–Co(1)–O(31)	92.42(12)	O(12)–Co(3)–O(67)	94.78(12)	O(10)–Co(6)–O(24)	94.34(12)	Co(1)–O(9)–Co(3)	97.11(12)
O(11)–Co(1)–O(13)	93.09(12)	O(12)–Co(3)–O(76)	177.01(12)	O(10)–Co(6)–O(51)	93.68(12)	Co(1)–O(9)–Co(5)	120.85(14)
O(11)–Co(1)–O(22)	176.32(12)	O(12)–Co(3)–O(85)	96.14(12)	O(10)–Co(6)–O(96)	95.49(12)	Co(2)–O(9)–Co(3)	97.21(12)
O(11)–Co(1)–O(31)	96.37(12)	O(67)–Co(3)–O(76)	86.12(12)	O(10)–Co(6)–N(124)	177.59(13)	Co(2)–O(9)–Co(5)	120.03(14)
O(13)–Co(1)–O(22)	87.43(12)	O(67)–Co(3)–O(85)	87.53(12)	O(24)–Co(6)–O(51)	118.78(13)	Co(3)–O(9)–Co(5)	119.57(14)
O(13)–Co(1)–O(31)	88.24(12)	O(76)–Co(3)–O(85)	86.75(12)	O(24)–Co(6)–O(96)	123.36(13)	Co(1)–O(10)–Co(2)	96.31(13)
O(22)–Co(1)–O(31)	87.29(12)	O(10)–Co(4)–O(11)	81.92(12)	O(24)–Co(6)–N(124)	86.16(13)	Co(1)–O(10)–Co(4)	97.44(13)
O(9)–Co(2)–O(10)	83.00(12)	O(10)–Co(4)–O(12)	81.78(12)	O(51)–Co(6)–O(96)	116.01(13)	Co(1)–O(10)–Co(6)	119.54(14)
O(9)–Co(2)–O(12)	82.40(12)	O(10)–Co(4)–O(94)	97.76(12)	O(51)–Co(6)–N(124)	88.14(14)	Co(2)–O(10)–Co(4)	97.77(12)
O(9)–Co(2)–O(40)	96.94(12)	O(10)–Co(4)–O(103)	176.82(12)	O(96)–Co(6)–N(124)	82.28(13)	Co(2)–O(10)–Co(6)	120.81(14)
O(9)–Co(2)–O(49)	174.25(11)	O(10)–Co(4)–O(112)	96.54(12)	O(11)–Co(7)–O(33)	97.47(12)	Co(2)–O(10)–Co(6)	119.65(14)
O(9)–Co(2)–O(58)	91.33(12)	O(11)–Co(4)–O(12)	82.35(12)	O(11)–Co(7)–O(78)	95.47(12)	Co(1)–O(11)–Co(3)	97.09(12)
O(10)–Co(2)–O(12)	82.18(12)	O(11)–Co(4)–O(94)	94.56(12)	O(11)–Co(7)–O(105)	95.94(12)	Co(1)–O(11)–Co(4)	97.99(13)
O(10)–Co(2)–O(40)	94.59(12)	O(11)–Co(4)–O(103)	97.17(12)	O(11)–Co(7)–O(127)	175.82(11)	Co(1)–O(11)–Co(7)	118.75(14)
O(10)–Co(2)–O(49)	96.01(12)	O(11)–Co(4)–O(112)	178.45(12)	O(33)–Co(7)–O(78)	118.01(13)	Co(3)–O(11)–Co(4)	97.20(13)
O(10)–Co(2)–O(58)	174.32(12)	O(12)–Co(4)–O(94)	176.90(12)	O(33)–Co(7)–O(105)	118.79(12)	Co(3)–O(11)–Co(7)	121.27(14)
O(12)–Co(2)–O(40)	176.75(12)	O(12)–Co(4)–O(103)	95.08(12)	O(33)–Co(7)–O(127)	85.45(12)	Co(4)–O(11)–Co(7)	119.42(14)
O(12)–Co(2)–O(49)	91.86(12)	O(12)–Co(4)–O(112)	97.50(12)	O(78)–Co(7)–O(105)	119.64(13)	Co(2)–O(12)–Co(3)	97.15(12)
O(12)–Co(2)–O(58)	97.49(12)	O(94)–Co(4)–O(103)	85.34(12)	O(78)–Co(7)–O(127)	85.74(12)	Co(2)–O(12)–Co(4)	97.44(12)
O(40)–Co(2)–O(49)	88.79(12)	O(94)–Co(4)–O(112)	85.59(12)	O(105)–Co(7)–O(127)	80.01(12)	Co(2)–O(12)–Co(8)	118.49(14)
O(40)–Co(2)–O(58)	85.70(12)	O(103)–Co(4)–O(112)	84.38(12)	O(12)–Co(8)–O(60)	95.59(11)	Co(3)–O(12)–Co(4)	96.62(13)
O(49)–Co(2)–O(58)	89.67(12)	O(9)–Co(5)–O(15)	94.70(12)	O(12)–Co(8)–O(87)	94.29(12)	Co(3)–O(12)–Co(8)	119.82(14)
O(9)–Co(3)–O(11)	82.41(12)	O(9)–Co(5)–O(42)	95.55(12)	O(12)–Co(8)–O(114)	94.11(12)	Co(4)–O(12)–Co(8)	121.92(14)

On the basis of the above considerations, the experimental magnetic susceptibility data were fit to the theoretical expression in eq 2,^{13–16} which describes the powder average χ_M vs T

$$\chi_M = \frac{Ng^2\mu_B^2}{3k(T - \Theta)} \left[\frac{9}{4} + \frac{3(1 - e^{-x})}{x(1 + e^{-x})} \right] + \text{TIP} \quad (2)$$

behavior for an $S = 3/2$ ion undergoing ZFS, where $x = 2D/kT$, N is Avogadro's number, D is the axial single-ion ZFS parameter, TIP is the temperature-independent paramagnetism, g_{\parallel} and g_{\perp} are taken to be equal, and the other symbols have their usual meaning. The Weiss constant (Θ) was included to account for the weak intramolecular and intermolecular $\text{Co}^{\text{II}} \cdots \text{Co}^{\text{II}}$ exchange interactions, which should only be of significance at the very lowest temperatures. The rhombic ZFS parameter (E) was taken as zero, given the effectively axial (C_{3v}) local symmetry at each Co^{II} ion. The fitting parameters were $|D| = 23.5(2.0) \text{ cm}^{-1}$, $\Theta = -1.76(8) \text{ K}$, and $g = 2.050(2)$, with TIP set at $700 \times 10^{-6} \text{ cm}^3 \text{ mol}^{-1}$ per Co^{II} . As has been noted in various other studies,^{14,18,19} powder susceptibilities are typically

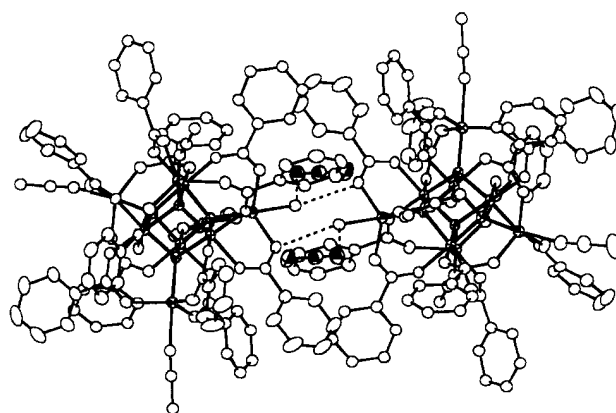


Figure 3. Arrangement of two molecules of **1b** showing the hydrogen-bonding interactions between the H_2O molecules and the carboxylate O and acetonitrile N atoms.

insensitive to the sign of D , and for complex **1a** similar quality fits to the data could be obtained with either positive or negative values of D . The TIP value employed is similar to that reported for a five-coordinate Co^{II} complex ($720 \times 10^{-6} \text{ cm}^3 \text{ mol}^{-1}$)¹³ and is also in the range reported for tetrahedral $[\text{CoX}_4]^{2-}$ ($X = \text{halide}$) complexes²⁰ ($(600\text{--}790) \times 10^{-6} \text{ cm}^3 \text{ mol}^{-1}$). Changing

(18) (a) Kennedy, B. J.; Murray, K. S. *Inorg. Chem.* **1985**, *24*, 1552. (b) Berry, K. J.; Clark, P. E.; Murray, K. S.; Raston, C. L.; White, A. H. *Inorg. Chem.* **1983**, *22*, 3928.

(19) Behere, D. V.; Mitra, S. *Inorg. Chem.* **1980**, *19*, 992.

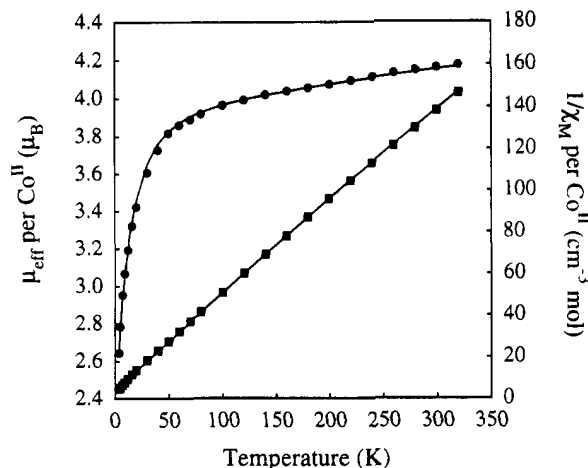


Figure 4. Plots of effective magnetic moment, $\mu_{\text{eff}}/\text{Co}^{\text{II}}$ (●), and the reciprocal of the molar magnetic susceptibility per Co^{II} , $1/\chi_M$ (■), versus temperature. The solid lines are derived from fits of the χ_M vs T data in the 4–320 K range to eq 2. See the text for the fitting parameters.

the TIP value has only a small effect on the obtained D value. The fit is shown as solid lines in Figure 4, where the data are plotted as μ_{eff} vs T and $(\chi_M)^{-1}$ vs T . It can be seen that the experimental data are well fit over the entire temperature range. The obtained value of D of 23.5 cm^{-1} is at the upper limit of values observed to-date for five-coordinate Co^{II} ($D = 7.0\text{--}25.3 \text{ cm}^{-1}$);^{13–16,21} these previous studies have involved Co^{II} centers in environments distinctly different from those in complex **1**, so detailed comparisons are unwarranted. In particular, none of the previous examples involved an oxide ligand.

If Θ is omitted from eq 2, the fit gives $|D| = 35.6(7) \text{ cm}^{-1}$ and $g = 2.045(2)$, with TIP set at $700 \times 10^{-6} \text{ cm}^3 \text{ mol}^{-1}$ per Co^{II} . The fit now does not reproduce the low-temperature data ($\leq 20 \text{ K}$); the experimental μ_{eff} values are smaller than the predicted values. The latter deviation is similar to that occasionally observed for mononuclear Co^{II} systems where it is a consequence of weak intermolecular exchange interactions that are antiferromagnetic in nature and cause the μ_{eff} values at very low temperatures to decrease faster than predicted from the ZFS alone. In one mononuclear Co^{II} complex exhibiting such behavior, the crystal structure indicated that hydrogen-bonded dimers were present, and fitting of the data to a model incorporating both ZFS and exchange interactions gave a good fit in the low-temperature region;¹⁴ the obtained parameters were $D = 7.0 \text{ cm}^{-1}$ and $J = -0.14 \text{ cm}^{-1}$. Ignoring the exchange interaction gave a higher apparent value of D (16.0 cm^{-1}). Complex **1b** (and presumably **1a**) also exists as hydrogen-bonded dimers; in this case, however, we have not pursued a fit including exchange interactions because of the *much* greater complexity arising from the octanuclear nature of the complex and the presence of both inter- and intramolecular interactions. Instead, we employed a Weiss constant (Θ) correction to T , and this gave the fitting parameters above and the solid lines in Figure 4. The negative value of Θ is consistent with antiferromagnetic exchange interactions in **1a**. Note that the obtained value of D for **1a** is also apparently higher (35.6 cm^{-1} vs 23.5 cm^{-1}) when no allowance is made for the weak exchange interactions.

Solution Studies. The paramagnetic nature of complex **1** indicated by the solid-state magnetic susceptibility studies on **1a** is also reflected in the solution ^1H NMR spectrum of **1c** in $(\text{CD}_3)_2\text{CO}$ shown in Figure 5. Only three paramagnetically-

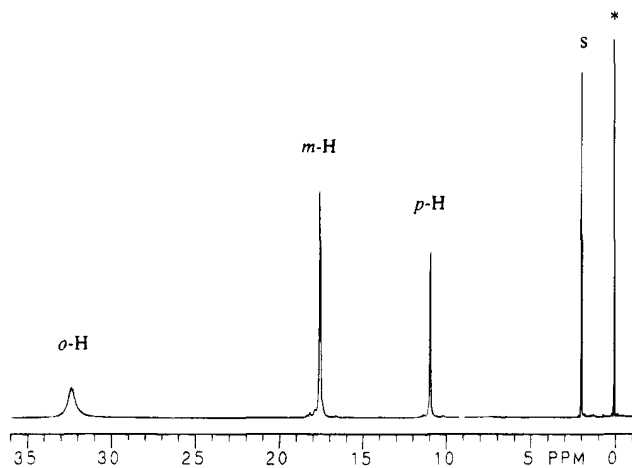


Figure 5. ^1H NMR (300 MHz) spectrum of complex **1c** in $(\text{CD}_3)_2\text{CO}$. The peaks marked with an asterisk and S are due to HMDS and solvent protio impurities, respectively.

shifted resonances are observed, at 32.32, 17.53, and 10.91 ppm at 296 K in a 2:2:1 integration ratio. The latter and the relative broadness of the peaks allow the assignments to benzoate hydrogen atoms indicated in the figure; the *ortho*-hydrogen is distinguished from the *meta*-hydrogen by its greater broadness, consistent with its closer proximity to the paramagnetic Co^{II} ions. A variable-temperature study in the range -90 to $+23$ °C shows standard Curie behavior; i.e., the paramagnetic shifts of the resonances from their diamagnetic positions increase with decreasing temperature. The simplicity of the spectrum in Figure 5 clearly indicates the presence of only one type of benzoate environment and is thus consistent with virtual T_d symmetry of the molecule in solution, the terminal MeCN/ H_2O groups presumably being replaced by $(\text{CD}_3)_2\text{CO}$ groups. This in turn indicates retention of the solid-state structure on dissolution in acetone. This is supported by the conductivity of **1c** in Me_2CO solution ($1 \text{ S}\cdot\text{cm}^2\cdot\text{mol}^{-1}$) that is clearly indicative of a nonelectrolyte. In CD_2Cl_2 or CD_3OD , the ^1H NMR spectra are essentially identical with the one in acetone. In particular, the spectrum of **1a** or **1c** in CD_2Cl_2 solution shows no evidence of the lower symmetry expected from the presence of two types of terminal solvent molecules (MeCN or DMF vs H_2O), suggesting that, within the resolution of the paramagnetically-broadened resonances, the magnetic environments of the carboxylate protons are not significantly affected by the identity of the terminal ligands.

The electrochemical properties of complexes **1a** and **1c** were examined by cyclic voltammetry (CV) and differential pulse voltammetry (DPV) in CH_2Cl_2 solution. Both complexes show only broad, ill-defined features in cathodic scans clearly due to irreversible reduction processes at approximately -0.4 and -1.2 V vs SCE. On the oxidation side, complex **1c** shows a quasi-reversible oxidation with a DPV peak potential of 1.54 V. The CV scans show well-shaped reverse waves in the 50–500 mV/s scan rate range explored. In this range, plots of i_p vs $\nu^{1/2}$ (ν = scan rate) give a straight line, indicating the oxidation to be a diffusion-controlled process. The couple is too close to the beginning of the solvent cutoff ($\sim 1.7 \text{ V}$) to allow coulometric studies, and it is thus assumed to be a one-electron process. Interestingly, complex **1a** does not display such a quasi-reversible oxidation process, the reverse peak in the CV scan being small and less well-defined. There is an additional

(20) Boudreaux, E. A.; Mulay, N. L. *Theory and Applications of Molecular Paramagnetism*; Wiley: New York, 1976.

(21) (a) Mäkinen, M. W.; Kuo, L. C.; Yim, M. B.; Wells, G. B.; Fukuyama, J. M.; Kim, J. E. *J. Am. Chem. Soc.* **1985**, *107*, 5245. (b) Mäkinen, M. W.; Kuo, L. C. *J. Am. Chem. Soc.* **1985**, *107*, 5255. (c) Mäkinen, M. W.; Yim, M. B. *Proc. Natl. Acad. Sci. U.S.A.* **1981**, *78*, 6221.

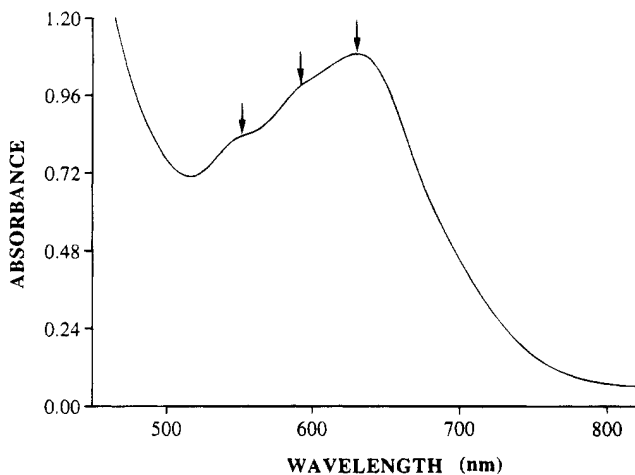


Figure 6. Electronic spectrum of **1a** in CH_2Cl_2 (6×10^{-1} mM) in the 450–820 nm region.

irreversible feature at *ca.* 1.3 V, however, in the region where DMF is oxidized, and it is thus possible that such prior ligand-based oxidations are the cause of the less reversible CV trace for **1a** in the *ca.* 1.5 V region. The value of 1.54 V vs SCE for the oxidation of **1c** is high and clearly demonstrates a resistance to oxidation of the Co^{II} ions; this rationalizes the isolation of a mixed-valence $\text{Co}^{\text{II}}/\text{Co}^{\text{III}}$ product in the preparative reactions for these complexes, even though a large excess of H_2O_2 was employed.

The electronic spectra of **1a** in CH_2Cl_2 (Figure 6) and MeOH look very similar. They are both quite rich, showing bands corresponding to transitions for octahedral low-spin d^6 Co^{III} and trigonal bipyramidal high-spin d^7 Co^{II} . Bands at 630 nm ($\epsilon_M = 1680 \text{ M}^{-1} \text{ cm}^{-1}$ per Co_8) and 592 (sh) in CH_2Cl_2 and at 620 nm ($\epsilon_M = 1050 \text{ M}^{-1} \text{ cm}^{-1}$) in MeOH are characteristic of high-spin Co^{II} in trigonal bipyramidal geometry and can be assigned to the ${}^4A_2'(F) \rightarrow {}^4A_2'(P)$ transition in D_{3h} symmetry or ${}^4A_{26}(F) \rightarrow {}^4A_2(P)$ in more-appropriate C_{3v} symmetry.^{22–24} From the calculations by Ciampolini,²⁵ it is apparent that the energy separation between the two levels ${}^4A_2'(F)$ and ${}^4A_2'(P)$ is not very sensitive to the strength of the ligand field, so bands at ~ 600 nm are diagnostic for trigonal bipyramidal Co^{II} . The presence of two bands at 630 and 592 nm is taken as reflecting the two different Co^{II} environments (varying in terminal MeCN or H_2O ligation) in poorly coordinating CH_2Cl_2 . The d–d bands at 552 nm (sh) and 568 nm (sh) in CH_2Cl_2 and MeOH, respectively, can be attributed to the ${}^1A_{1g} \rightarrow {}^1T_{1g}$ transition for Co^{III} in O_h symmetry since the same transition appears in this region for the cubane complexes $[\text{Co}_4\text{O}_4(\text{O}_2\text{CR})_2(\text{bpy})_4](\text{ClO}_4)_2$

($R = \text{CH}_3, \text{CH}_3\text{C}_6\text{H}_4$). A broad shoulder at ~ 500 nm in MeOH can tentatively be assigned to the ${}^4A_2'(F) \rightarrow {}^4E''(P)$ transition for Co^{II} . All of the above bands obey Beer's law in the concentration range 0.25–1.0 mM in both CH_2Cl_2 and MeOH, again supporting retention of the structure on dissolution. Strong charge transfer bands appear at 328 nm (sh) and 340 nm in CH_2Cl_2 and MeOH, respectively.

Discussion

There are several noteworthy points about the described work and some interesting conclusions that can be drawn. The isolation of a mixed-valence $\text{Co}^{\text{II}}/\text{Co}^{\text{III}}$ species from a reaction involving an excess of H_2O_2 is somewhat surprising but can be rationalized by its resistance to oxidation as indicated in the electrochemical studies. Although the mechanism of assembly of the product is unknown, this suggests (i) that the rate of formation of complex **1** must be comparable with the rate of oxidation of mononuclear Co^{II} and (ii) that once formed, the complex retains its structure in solution, as supported by the conductivity measurements and the ${}^1\text{H}$ NMR and electronic spectra.

The structure itself is remarkable for a molecular species and shows that even an oxide bridging three tripositive Co centers retains enough basicity to bind to a fourth Co ion. As we have described elsewhere, this suggests that other Lewis acids, such as H^+ ions, might also be capable of attaching to the $\mu_3\text{-O}^{2-}$ ions of a $[\text{Co}_4\text{O}_4]^{4+}$ cubane: indeed, the protonated cores $[\text{Co}_4\text{O}_3(\text{OH})]^{5+}$ and $[\text{Co}_4\text{O}_2(\text{OH})_2]^{6+}$ have been obtained by treatment of $[\text{Co}_4\text{O}_4(\text{O}_2\text{CR})_2(\text{bpy})_4]^{2+}$ with strong acids.⁵ These combined results further suggest that other $[\text{M}_4\text{O}_4]$ cubanes may also find use as starting points for controlled conversion to higher nuclearity products or to protonated versions.

The effective magnetic moment of complex **1a** is very temperature-dependent, and the described studies indicate that this is due to ZFS of the spin quartet ground state of the Co^{II} ions. Evidence for inter- and intramolecular exchange interactions is present, but it is concluded that these effects are minor ($< 1 \text{ cm}^{-1}$) relative to the ZFS. Thus, the $[\text{Co}_4\text{O}_4]^{4+}$ core, which can reasonably be described as functioning as a quadruply-bridging unit, is able to mediate only a very weak exchange interaction between the Co^{II} ions.

Finally, we stated in the Introduction that it was our suspicion that Co carboxylate chemistry might prove a rich area for what is otherwise a well-studied metal. The described results, together with those previously reported at the tetranuclear level and a variety of unpublished results, seem to suggest that our suspicions were correct.

Acknowledgment. This work was supported by NSF Grant CHE 9311904.

Supporting Information Available: Textual and tabular details of data collection and refinement, complete listings of atomic coordinates, thermal parameters, bond distances, and bond angles, and a fully labeled figure (26 pages). Ordering information is given on any current masthead page.

IC9414278

(22) Lever, A. B. P. *Inorganic Electronic Spectroscopy*, 2nd ed.; Elsevier: Amsterdam, 1984; p 491.

(23) Banci, L.; Bencini, A.; Benelli, C.; Gatteschi, D.; Zanchini, C. *Struct. Bonding (Berlin)* **1982**, 52, 37.

(24) Dori, Z.; Gray, H. B. *Inorg. Chem.* **1968**, 7, 889.

(25) Ciampolini, M.; Nardi, N.; Speroni, G. P. *Coord. Chem. Rev.* **1966**, 1, 222.